ISSN 2349-4506
Impact Factor: 2.265

Global Journal of Engineering Science and Research Management

THERMOPLASTIC ANALYSIS OF FUNCTIONALLY GRADED ROTATING DISCS WITH VARIABLE THICKNESS UNDER THERMO-MECHANICAL LOADING AND UNLOADING

Eqlima Mahdavi*
*Iran University of Science and Technology, Narmak, Tehran, 16846-13114, Iran.

KEYWORDS: A. functionally graded rotating disk; B. unloading behavior; B. Residual/internal stress; C. variable material property theory; C. Finite element analysis (FEA).

ABSTRACT

This work presents an analysis of the thermo-mechanical behavior of rotating discs made of functionally graded material (FGM) with variable thickness and constant angular velocity. The solutions are obtained by variable material property (VMP) theory. In this theory, the domain is divided into some finite sub-domains in the radial direction, in which the thermo-mechanical properties are assumed to be constant and the form of the elastic response is used to solve elastic-plastic problems. The results obtained by the VMP method are then compared with the results obtained by the finite element analysis using ANSYS software. In addition, the unloading and reverse yielding behavior of FG rotating disk are investigated and the residual stresses are then calculated with the same values of pressure and temperature by VMP theory and FE analysis. The results reveal that the mentioned methods are in very good agreement in both elastic and elasto-plastic states.

Subsequently, the effect of various parameters including the disk geometry, temperature distribution, angular velocity, and boundary conditions on the stress behavior of disk is investigated. The results show that unlike the uniform rotating discs in which the yielding necessarily initiates from the inner radius, in the FG rotating discs, plasticity can be initiated from any point..

INTRODUCTION

Functionally graded materials (FGMs) are a new type of advanced composites, which have been used for many engineering applications. The main application of FGMs is in high temperature such as automotive, aircrafts, turbine rotors, flywheels, gears etc. In these materials, the volume fraction of the two or more materials is varied steadily and non homogeneously as a function of position along thickness [1, 2]. Usually, a ceramic is used at the outer surface and a metal is used to another surface, which the volume fraction changes steadily. Within FGMs the different microstructural phases have different functions, and the overall FGMs attain the multi-structural status from their property gradation. By gradually varying the volume fraction of constituent materials, their material properties exhibit a smooth and continuous change from one surface to another [3].

Noda and Tsuji [4] and Obata et al. [5] considered thermal load in a plate made of FGMs. Tanaka et al. [6, 7], Yongdong et al. [8], and Zhong and Yu [9] studied the analysis of stress due to mechanical loads in FGM beams. Ravichandran [10] calculated the thermal residual stresses of an FGM material system.

Rotating discs are widely used in various applications in aerospace industries such as gas turbines, jet engines, flywheels, cars, pumps, compressors etc. Rotating discs are usually operating at high angular velocities and subjected to thermo-mechanical loadings. Recent studies have shown that, at the same angular velocity, the stresses developed in a rotating disk (hollow or solid) with variable thickness are much lower than those of a disk with uniform thickness are. Gamer [11, 12] investigated a solution for a constant thickness rotating disk.

G*ü*ven [13, 14] studied the fully plastic rotating disk with variable thickness and the applicability of Tresca's yield condition to the linear hardening rotating solid disk with variable thickness.

Duva et al. [15] studied the characteristic of FGM disk and strain suppression at stress concentrators. Ha et al. [16] investigated the stress distribution in flywheels with functionally graded material under plane strain conditions. Zenkour [17] has showed analytical solutions for rotating FGM annular discs with various boundary conditions. Durodola and Attia [18] studied deformation and stresses in FG rotating discs. Naghdabadi and Hosseini Kordkheili [19] have derived a finite element formulation for the thermo-elastic analysis of FG plates and shells. They assumed the power-law distribution model for the composition of the constituent materials in shell thickness direction.

Bayat et al. [20] implemented a semi-analytical method to elastic analysis of functionally graded rotating disk with variable thickness (see Fig. 1). The material properties and disk thickness profile are assumed to be presented

by two power-law distributions. Results revealed that, in functionally graded rotating disk with parabolic or hyperbolic convergent thickness profile, stresses and displacements are smaller than that with uniform thickness profile.

Afsar and Go [21] concentrated on the finite element analysis of thermo-elastic field in a thin circular functionally graded material (FGM) disk subjected to a thermal load and an inertia force due to the rotation of disk. Their analysis shows that the thermo-elastic field in such disk is seriously affected by temperature distribution profile, thickness of the disk, and angular velocity.

Jahed and Shirazi [22] investigated the effect of loading, residual stress, displacements, and associated strain for rotating discs at elevated temperature.

Jahed and Dubey [23] proposed an axisymmetric method for elastic plastic analysis of rotating disk. Farshi et al. [24] obtained an optimum profile for rotating disk with plastic deformation by variable material properties theory (VMP).

In this paper, stresses and strains are obtained in rotating discs made of functionally graded materials with variable thickness under thermo-mechanical loading and residual stresses are then calculated under mechanical unloading. The results obtained by the VMP method are then compared with the results obtained by the finite element analysis using ANSYS software. These comparisons show that the results from the VMP method are in good agreement with FE analysis, thus verifying the reliability and accuracy of the VMP theory. Next, ν_{eff} and E_{eff} , the effective Poisson's ratio and effective Young's modulus by VMP method are investigated.

Finally, the effects of the boundary conditions, temperature gradient, angular velocity, and thickness profile on the stress behavior of disk are investigated by the VMP method.

MATHEMATICAL MODEL

Gradation relation

Several FGMs are manufactured by two phases of materials with different properties. A detailed description of actual graded microstructures is usually not available, except perhaps some information on the volume fraction distribution. Since the volume fraction of each phase gradually varies in the gradation direction, the effective properties of FGMs change along this direction [3].

A functionally graded rotating disk (inner radius r_i , outer radius r_o , and angular velocity ω) made by mixing two distinct material phases, for example a metal and a ceramic, is considered with Cylindrical polar coordinates *r*, θ, and *z* (see Fig. 1). It is assumed that, the volume fraction of metal and ceramic follow a simple power law:

$$V_m = \left(\frac{r - r_i}{r_o - r_i} \right)^N , \quad V_c = 1 - V_m \tag{1}$$

where V_C and V_m are the volume fractions of ceramic and metal, respectively and the volume fraction index N dictates the material variations profile through the FGM.
So, the effective material properties of the FGM layer, P_f , such as Young's modulus, Poisson's ratio, thermal expansion coefficient, density, yield strength, and tangent modulus can then be expressed as:

$$P_f = P_m V_m + P_C V_C \tag{2}$$

where P_m and P_C are the material properties of ceramic and metal, respectively.

The Disk Model

The thickness profile of disk is assumed vary radially in a form given by

$$h(r) = h_o \left(\left(\frac{r}{r_o} \right)^{-m} \right)$$

(3) where m and h_o are geometric parameters. m can be negative or positive and h_o is the thickness at the axis of the disk.

Different forms of thickness profile of disk with negative, zero, and positive values of m are shown in Fig. 2. It can be seen that the profile is convergent for $m > 0$ and divergent for $m < 0$. By considering $m = 0$, constant thickness is obtained.

FORMULATION OF THE PROBLEM

Governing equations

Despite the thickness and properties of the rotating disk, the relations between the radial displacement, u, and the strains are

$$\varepsilon_r = \frac{du}{dr}, \quad \varepsilon_\theta = \frac{u}{r} \tag{4}$$

where ε_r and ε_θ are the total radial and hoop strain, respectively.

For disk with cylindrical coordinate system, the stress components are defined on the differential element shown in Fig. 3.

Because the thickness of disk is considered to be small in comparison with its diameter, the problem is assumed to be plane stress. On the other hand, the inertia force due to the angular velocity of the disk is the only body force and because of symmetry, $\tau_{r\theta}$ vanishes. Thus, the equilibrium equation is reduced to [25]

$$\frac{d}{dr}(hr\sigma_r) - h\sigma_\theta + \rho h r^2 \omega^2 = 0 \tag{5}$$

where h, σ_r, and σ_θ are thickness, radial stress, and hoop stress, respectively.

The deformation of the rotating disk consists of three components: elastic (ε^e), plastic (ε^p), and thermal (ε^T) strains. Total strains are the sum of these components:

$$\varepsilon_{ij} = \varepsilon_{ij}^e + \varepsilon_{ij}^p + \varepsilon_{ij}^T \tag{6}$$

$$\varepsilon_{ij}^e = ((1+\nu)\sigma_{ij} - \nu\sigma_{kk}\delta_{ij})/E, \tag{7}$$

$$\varepsilon_{ij}^p = \phi(\sigma_{ij} - \delta_{ij}\sigma_{kk}/3), \quad \phi = 3\varepsilon_{eq}^p/2\sigma_{eq} \tag{8}$$

$$\varepsilon_{ij}^T = \alpha\Delta T \tag{9}$$

ε_{eq}^p is the equivalent plastic strain and σ_{eq} is the equivalent stress. In this work, analysis is based on von Mises yield criterion and σ_{eq} is given by:

$$\sigma_{eq} = \sqrt{\sigma_r^2 + \sigma_\theta^2 - \sigma_r\sigma_\theta} \tag{10}$$

Eq. (6) can be rewritten in the following form:

$$\varepsilon_{ij}^{tot} = \frac{1+\nu_{eff}}{E}\sigma_{ij} - \frac{\nu_{eff}}{E_{eff}}\sigma_{kk}\delta_{ij} + \alpha\Delta T \tag{11}$$

The materials is assumed to follow an elastic linear hardening [25] model for the stress–strain relationship (see Fig. 4).

$$\begin{cases} \varepsilon = \dfrac{\sigma}{E} & \sigma \le \sigma_0 \\ \varepsilon = \dfrac{\sigma_0}{E} + \dfrac{1}{E_t}(\sigma - \sigma_0) & \sigma > \sigma_0 \end{cases} \tag{12}$$

where σ_0 and E_t are the yield strength of the material and tangent modulus, respectively.

Therefore, following relation is obtained for total strain:

$$\varepsilon_{ij}^{tot} = \left(\frac{1+\nu}{E}+\phi\right)\sigma_{ij} - \left(\frac{\nu}{E}+\frac{1}{3}\phi\right)\sigma_{kk}\delta_{ij} + \alpha\Delta T \quad (13)$$

Here, ν_{eff} and E_{eff}, the effective Poisson's ratio and effective Young's modulus, depend on the final state of stress at a point and given by [22]

$$E_{eff} = \frac{3E}{3+2E\phi}, \quad \nu_{eff} = \frac{3\nu+E\phi}{3+2E\phi} \quad (14)$$

Variable material property theory

In variable material property theory, the domain is divided into some finite uniform sub-domains in the radial direction (see Fig. 5), each annulus having the constant thermo-mechanical properties and boundary conditions with internal and external pressures as well as temperatures. Then, the form of the elastic response is used to solve elastic-plastic problems [22].

For this purpose, first, we should obtain the thermoelastic solution of the disk.

For each rotating annulus with constant mechanical and physical properties and uniform thickness with plane stress condition, the elastic solution is Lame's solution [25]:

$$u(r) = \left[m_1 r + \frac{m_2}{r}\right] + \left[n_1 r + \frac{n_2}{r} - \frac{1-\nu^2}{8E}\rho r^3\omega^2\right] + \left[(1+\nu)rJ(r) + (1-\nu)Ir + r_1^2(1+\nu)\frac{I}{r}\right] \quad (15)$$

in which

$$m_1 = \frac{1-\nu}{Eh\left(r_1^2-r_2^2\right)}\left(F_2 r_2^2 - F_1 r_1^2\right),$$

$$m_2 = \frac{(1+\nu)r_1^2 r_2^2}{Eh\left(r_1^2-r_2^2\right)}\left(F_2 - F_1\right),$$

$$n_1 = \frac{(1-\nu)(3+\nu)}{8E}\rho\omega^2\left(r_1^2+r_2^2\right),$$

$$n_2 = \frac{(1+\nu)(3+\nu)}{8E}\rho\omega^2\left(r_1^2 r_2^2\right),$$

$$I = \frac{1}{r_2^2-r_1^2}\int_{r_1}^{r_2} r\alpha T \; dr,$$

$$J(r) = \frac{1}{r^2}\int_{r_1}^{r} r\alpha T \; dr.$$

where E, ν, and ρ are the mechanical and physical properties of each annulus, ω is the angular velocity of disk, h is the uniform thickness of each annulus, r_1 and r_2 are the inner and outer radiuses, F_1 and F_2 are the internal and external forces, and T is the temperature profile in each annulus.

By setting $r = r_1$ and $r = r_2$, u_1 (displacement at inner radius of each annulus) and u_2 (displacement at outer radius of each annulus) can be obtained, respectively.

On the other hand, boundary conditions of disk are continuity of displacements and forces in common radiuses of neighbor strips and total boundary conditions of disk, namely:

$$\begin{cases} u(r_2^{(k)}) = u(r_1^{(k+1)}) \\ F(r_2^{(k)}) = F(r_1^{(k+1)}) \end{cases}$$

$$\begin{cases} \sigma_r = 0; & r = r_i \\ \sigma_r = 0; & r = r_o \end{cases} \qquad (16)$$

$$r_1^{(k)} = r^{(k)} - \frac{t^{(k)}}{2}, \quad r_2^{(k)} = r^{(k)} + \frac{t^{(k)}}{2}$$

in which $r^{(k)}$ and $t^{(k)}$ are the mean radius and width of kth strip, respectively.

By using above matrix equations for each strip and boundary conditions at interior and exterior radiuses of each annulus and the disk, a system of linear equations is constituted. By solving this system of equations, displacements and forces at boundaries of each strip will be obtained.

After obtaining the forces in each layer, radial and hoop stresses can be determined by:

$$\sigma_{rr} = \left[A_1 - \frac{A_2}{r^2}\right] + \frac{3+\nu}{8}\rho\omega^2\left[r_2^2 + r_1^2 - \frac{r_1^2 r_2^2}{r^2} - r^2\right] + E\left[-J(r) + I\left(1 - \frac{r_1^2}{r_2^2}\right)\right]$$

$$\sigma_{\theta\theta} = \left[A_1 + \frac{A_2}{r^2}\right] + \frac{3+\nu}{8}\rho\omega^2\left[r_2^2 + r_1^2 + \frac{r_1^2 r_2^2}{r^2} - \frac{1+3\nu}{3+\nu}r^2\right] + E\left[J(r) - \alpha T(r) + I\left(1 + \frac{r_1^2}{r_2^2}\right)\right] \qquad (17)$$

in which A_1 and A_2 are determined as follows:

$$A_1 = \frac{F_2 r_2^2 - F_1 r_1^2}{\left(r_1^2 - r_2^2\right)h}, \quad A_2 = \frac{\left(F_2 - F_1\right)r_1^2 r_2^2}{\left(r_1^2 - r_2^2\right)h}$$

Thermal loading are assumed in this form:

$$T(r) = A\ln\left(\frac{r}{r_o}\right) + T_o, \quad A = \frac{T_i - T_o}{\ln(r_i / r_o)} \qquad (18)$$

To employ the VMP method, E_{eff} and ν_{eff} should be substituted in the relations of elastic solution.

Calculation of E_{eff} and n_{eff}

To evaluate the E_{eff} and ν_{eff} in each strip, an iterative manner is used [22]. This iterative manner will be continued until the $\sigma_{eq} - \varepsilon_{eq}$ matches on the true stress-strain curve with a small tolerance. There are three schemes to evaluate the spatial distribution of E_{eff} and ν_{eff} : (a) Projection method, (b) Arc-length method, and (c) Neuber's rule [22].

In this study, projection method is used to update the E_{eff} and ν_{eff} . In this method, as shown in Fig. 6, first, after obtaining the elastic solution of disk and comparing of equivalent stress and yield stress, if σ_{eq} is greater than σ_0 (yield stress), point "a" is developed in true stress-strain curve. From point "a" with the same value of strain, point "a'" is produced by projecting on curve of plastic region of material. Then, new E_{eff} is determined by $(E_{eff})_{new} = (\sigma)_{a'}/(\varepsilon)_{a'}$. By using new E_{eff} , this procedure will be continued until the $\sigma_{eq} - \varepsilon_{eq}$ matches on true stress-strain curve with a small tolerance. It should be noted that if σ_{eq} is smaller than yield stress, previous determined E_{eff} and ν_{eff} should be used.

Execution of unloading process

As soon as the angular velocity reduces, unloading happens in the disk. To evaluate the unlodaing stresses, a new process is developed in which the thermo-mechanical conditions are the same as that in loading process. However, the material stress-strain curve is changed because of different material behaviour in loading and unloading processes.

The conventional bilinear model with kinematic hardening is plotted in Fig. 7. The reverse yielding in the process of unloading occures when the stress value reaches the value σ_{0U} defined by:

$$\sigma_{0U} = 2\sigma_0 \tag{19}$$

Introduced the unloading curves for each annulus and by using the same manner described in the loading process with the same thermo-mechanical boundary condition, the unloading behavoiur is determined.
Then, the residual hoop and radial stresses following unloading process is obtained as follows:

$$\begin{cases} \sigma_R^R = \sigma^R - \sigma_U^R \\ \sigma_R^H = \sigma^H - \sigma_U^H \end{cases} \tag{20}$$

in which σ^R and σ^H are the radial and hoop stresses, respectively, in loading process and σ_U^R and σ_U^H are the corresponding stresses obtained from the unloading analysis.

FINITE ELEMENT ANALYSIS

In the analysis of the disk, which thickness is small in comparison with its diameter, plane stress condition is considered. In finite element analysis, commercially availabe software, ANSYS, is employed [26]. 2-D structural solid elements (PLANE42) are used to modeling of the disk. Subsequently, the results of the finite element model are compared with the results of VMP method.

RESULTS AND DISCUSSION

For numerical illustrations, one set of material mixture is considered for an FGM rotating disk. The inner radius of the FGM rotating disk is metal-rich and the outer radius is ceramic-rich. Material properties of constituents in the inner and outer radiuses are presented in Table 1, referred to as mat_1 and mat_2, respectively. For this example, the disk geometric parameters are $r_i = 0.1\,\mathrm{m}$ and $r_o = 0.5\,\mathrm{m}$ as the inner and outer radiuses, respectively. Thickness profile is assumed to be nonlinear function of radius value of eq. (3), with $h_o = 0.02$ and $m = 0.5$. $T_i = 0°\mathrm{C}$ and $T_o = 350°\mathrm{C}$ are considered as a thermal conditions at the inner and outer radiuses, respectively. Variation of temperature profile through the radius of hollow disk due to steady state temperature is depicted in Fig. 8. The temperature field is assumed to be the same as eq. (18). Because of higher temperature at the outer radius, the outer surface of disk is ceramic-rich.

In this study, the thickness of the disk in comparison with its diameter is small, so plane stress condition can be employed.

We first study the convergence of the VMP theory and FE analysis for the given properties between the inner and the outer surface of the disk with free-free boundary condition and $\omega = 500\ \mathrm{rad/sec}$. It's find that for n=50 (number of divisions), in VMP theory and FE analysis, the responses are converged.

Then, in Figs. 9 and 10, the effective Young's modulus and effective Poisson's ratio in the radial direction are plotted by using VMP theory. In these figures, we compared the Young's modulus and effective Young's modulus as well as Poisson's ratio and effective Poisson's ratio. As mentioned before, if the disk in certain radius of its domain does not inter to plastic region, the effective Young's modulus and the Young's modulus will be the same. Then, by use of these values for effective Young's modulus and effective Poisson's ratio, the results obtained from VMP theory and FE analysis are presented and compared in Figs. 11 and 12 for loading and unloading radial and hoop stresses, respectively. As observed in these figures, these two methods are in good agreement. Maximum difference between them for radial and hoop stresses are 3.2% and 4%, respectively.

In addition, radial displacement of the disk are plotted in Fig. 13. Clearly, the comparison is reasonably well and the maximum difference between two methods is 0.16%.

The effect of temperature gradient on the effective Young's modulus, radial stress, and hoop stress has been shown in Figs. 14-16, respectively. For simplicity of numerical calculations, the temperature at the inner surface remains unchanged, i.e. $T_i = 0°C$; and the temperature at the outer surface is changed.

The previous research on the uniform rotating disk reveals that the yielding initiates from the inner radius [25], while as is presented in Fig. 14, plasticity in FG disk could be initiated at any point.

From Fig. 15, it can be seen that in lower temperature gradient, the value of hoop stress at the inner radius are larger than that at the outer radius and with increases in temperature gradient, the maximum value of hoop stress occurs at the outer surface of the disk. Furthermore, there exists two points on the domain, i.e., $r \approx 0.216\text{m}$ and $r \approx 0.46\text{m}$ in which the changes in the temperature gradient have no effect on the hoop stresses.

From Fig. 16, it is found that the radial stresses increase as the temperature gradient between the inner and outer surfaces of the disk increases; and the location of maximum stress approaches to the inner radius. It can also be seen that radial stresses have the same value at $r \approx 0.4\text{m}$. That means there is an interior radius in the disk in which the temperature gradient has the least effect on radial stresses. Passing through this point, the effect of temperature gradient on radial stress reverses.

Figs. 17-19 give the effect of different profile thickness on the effective Young's modulus, radial stresses, and hoop stresses with changing m in Eq. (3). As mentioned before, in the hyperbolic profile as Eq. (3), for $m < 0$, the profile is divergent and for $m > 0$, the profile is convergent. The constant thickness is obtained for $m = 0$.

It can be seen that from Fig. 17, the most plastic region occurs in the disk with $m = -1$ (divergent profile) and disk with $m = 1$ (convergent profile) have the minimum plastic region. Moreover, it can be concluded that the plastic area decreases as m increases.

Fig. 18 shows that the disk with divergent or convergent profile has smaller maximum radial stress than that with constant thickness. It can also be seen that for both divergent and convergent thickness profile of disk, the radial stress decreases as the order of hyperbola, m, increases.

It is evident from Fig. 19 that in the disk with convergent profile, hoop stress is lower than that in the disk with divergent profile, as well as constant profile. In addition, the difference of hoop stresses between the inner and outer radiuses is lower for the disk with $m = 1$. It means that the disk with convergent thickness have more smooth stress distribution.

Then, the effect of the angular velocity on the disk is investigated. The obtained results for radial and hoop stresses along the radius of disk are plotted in Figs. 20 and 21, respectively.

As it is expected, the radial stresses (see Fig. 20) increases as the angular velocity increases which is due to its direct effect on the body force and the changes are significant. Furthermore, in low angular velocity, radial stress is compressive around the outer radius of disk. It can also be seen that the change in angular velocity moves the location of maximum radial stress outward. Whereas the maximum value of hoop stress is located at the inner radius for each angular velocity value (see Fig. 21). Furthermore, as the angular velocity increases, difference of hoop stresses between the inner and outer radiuses is increased significantly.

Finally, we present the influence of different boundary conditions on the stresses. Boundary condition of the disk depends on the way that the disk is attached to the shaft. For this purpose, four sets of boundary condition, i.e. free-free, free-free with internal pressure ($P_i = 100\text{MPa}$), clamped-free, and clamped-clamped are considered at the inner and outer surfaces of disk. Fig. 22 shows that the disk with clamped-clamped boundary condition has the most plastic part while that one with free-free boundary condition has the least plastic region. Furthermore, from Fig. 23, it can be seen that the disk with clamped-clamped edge boundary condition has the highest maximum compressive radial stress and the disk with clamped-free boundary condition has the highest maximum

tensile stress. In addition, Fig. 24 shows that the disk under the effect of internal pressure has the highest tensile hoop stress and that one with clamped-clamped boundary condition undergoes the highest maximum compressive hoop stress.

CONCLUSIONS

In this paper, thermoplastic analysis of functionally graded rotating disk with variable thickness is solved by using the variable material property theory. In this theory, the elastic response is used to solve the inelastic problem, with substitution appropriate effective Young's modulus that obtained from true stress-strain curve. The unloading behavior of disk is also obtained in the same manner. The results obtained by the VMP method are then compared with the results obtained by the finite element analysis using ANSYS software. The results reveal that mentioned methods are in very good agreement in both elastic and plastic states.

Finally, the effect of temperature gradient, the order of thickness profile, angular velocity, and boundary conditions on the stress behavior of disk was investigated. The results show that these parameters have significant effects on stress behavior of the discs and the discs with variable thickness profile have smaller stresses than those with constant thickness. Moreover, it can be found that unlike the uniform rotating discs in which the yielding necessarily initiates from the inner radius, in the FG rotating discs, plasticity can be initiated from any point.

REFERENCES

[1] Suresh S, Mortensen A. Fundamentals of functionally graded materials. London: Institute of Materials (IOM) Communications Limited; 1998.
[2] Reddy JN. Analysis of functionally graded plates. Int J Numer Methods Eng 2000;47:663–84.
[3] Hui-shen shen. Functionally graded materials: Nonlinear analysis of plates and shells.Taylor & Francis Group, Boca roton; 2009.
[4] Noda N, Tsuji T. Steady thermal stresses in a plate of functionally gradient material with temperature-dependent properties. Trans Jpn Soc Mech Eng Ser A 1991;57:625–31.
[5] Obata Y, Noda N, Tsuji T. Steady thermal stresses in a functionally gradient material plate. Trans Jpn Soc Mech Eng 1992;58:1689–95.
[6] Tanaka K, Tanaka Y, Enomoto K, Poterasu VF, Sugano Y. Designof thermo elastic materials using direct sensitivity and optimization methods, reduction of thermal stresses in functionally gradientmaterials. Comput Methods Appl Mech Eng 1993;106:271–84.
[7] Tanaka K, Tanaka Y, Watanabe H, Poterasu VF, Sugano Y. Animproved solution to thermo elastic material design in functionally gradient materials: scheme to reduce thermal stresses. ComputMethods ApplMech Eng 1993;109:377–89.
[8] Yongdong L, Hongcai Z, Nan Z, Yao D. Stress analysis of functionally gradient beam using effective principal axes. Int J Mech Mater Des 2005;2:157–64.
[9] Zhong Z, Yu T. Analytical solution of a cantilever functionally graded beam. Compos Sci Technol 2007;67:481–88.
[10] Ravichandran KS. Thermal residual stresses in a functionally graded material system. Mater Sci Eng A 1995;201: 269–76.
[11] Gamer U. Elastic–plastic deformation of the rotating solid disk. Ingenieur-Archiv 1984;54:345–54.
[12] Gamer U. Stress distribution in the rotating elastic–plastic disk. ZAMM 1985;65:T136–7.
[13] Güven U. The fully plastic rotating disk of variable thickness. ZAMM 1994;74:61–5.
[14] Güven U. On the applicability of Tresca's yield condition to the linear hardening rotating solid disk of variable thickness. ZAMM 1995;75:397–8.
[15] Duva JM, Olson BR, Wadley HNG. Functionally graded materials for strain suppression at stress concentrators. Compos Eng 1994;4(1):107–14.
[16] Ha SK, Yoon Y, Han SC. Effects of material properties on the total stored energy of a hybrid flywheel rotor. Arch Appl Mech 2000;70:571-84.
[17] Zenkour AM. Analytical solutions for rotating exponentially-graded annular disks with various boundary conditions.Int J Struct Stab Dynam 2005;5:557-77.
[18] Durodola JF, Attia O. Deformation and stresses in FG rotating disks. Compos SciTechnol 2000;60:987–95.
[19] Kordkheili SAH, Naghdabadi R. Thermoelastic analysis of a functionally graded rotating disk ComposStruct 2007; 79:508-16.
[20] Bayat M, Saleem M, Sahari BB, Hamouda AMS, Mahdi E. Analysis of functionally graded rotating disks with variable thickness. Mechanics research Communications 2008;35:283-309.

[21] Afsar AM, Go J. Finite element analysis of thermoelastic field in a rotating FGM circular disk. Aplied Mathematical Modelling 2010;34:3309–20.
[22] Jahed H, Shirazi R. Loading and unloading behaviour of a thermoplastic disc. International Journal of Pressure Vessel and Piping 2001;78:637–45.
[23] Jahed H, Dubey RN. An axisymmetric method of elastic plastic analysis capable of predicting residual stresses. J Pressure Vessel Technol 1997;119:264–73.
[24] Farshi B, Jahed H, Mehrabian A. Optimum design of inhomogeneous nonuniform rotating discs. Comput Struct 2004;82:773–9.
[25] Timoshenko SP, Goodier JN. Theory of elasticity.3rd ed. McGraw-Hill New York; 1970
[26] User's manual of ANSYS 10.0. ANSYS Inc; 2005.

FIGURES

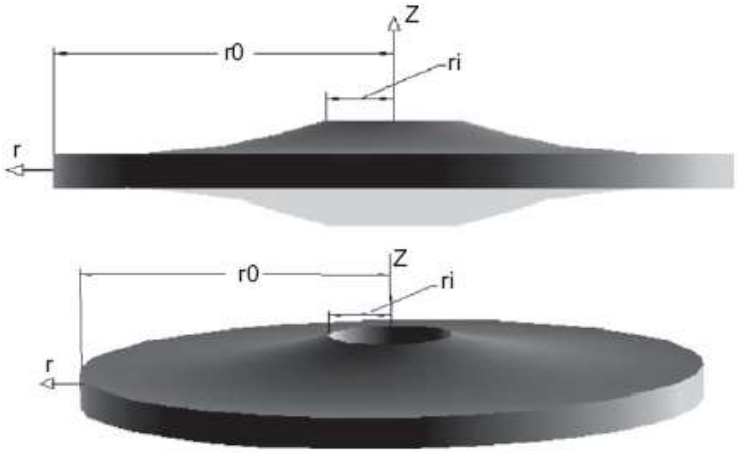

Fig. 1. Configuration of a thin disk with variable thickness [20].

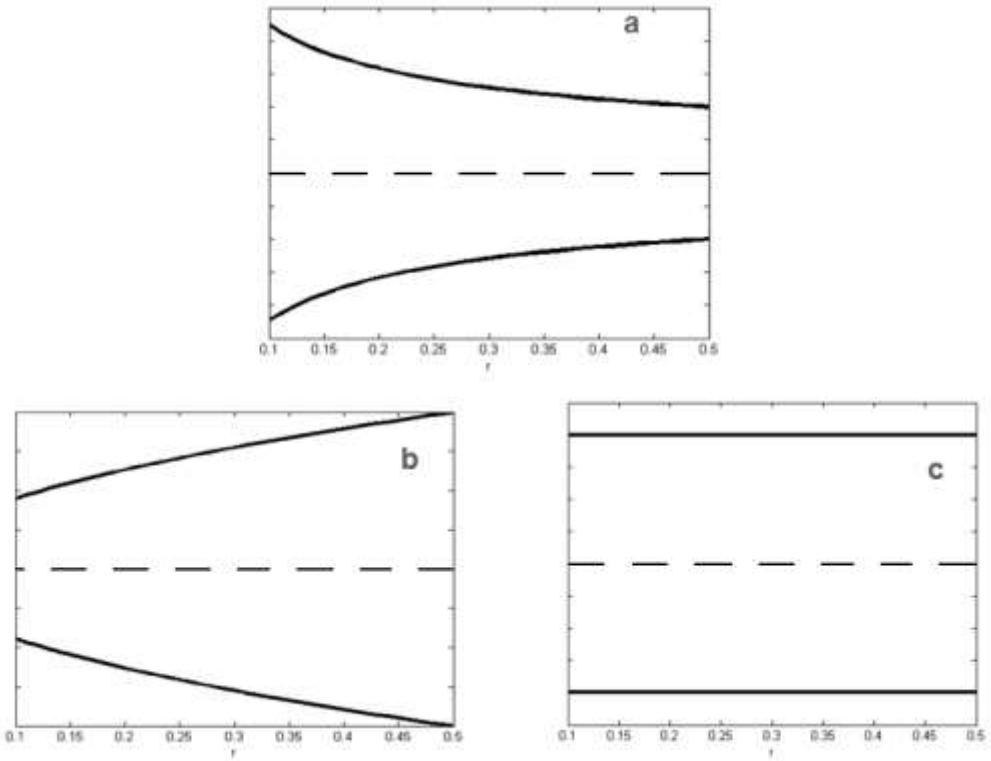

Fig. 2. Thickness profile of disk (a) convergent, (b) divergent, and (c) constant.

ISSN 2349-4506
Impact Factor: 2.265

Global Journal of Engineering Science and Research Management

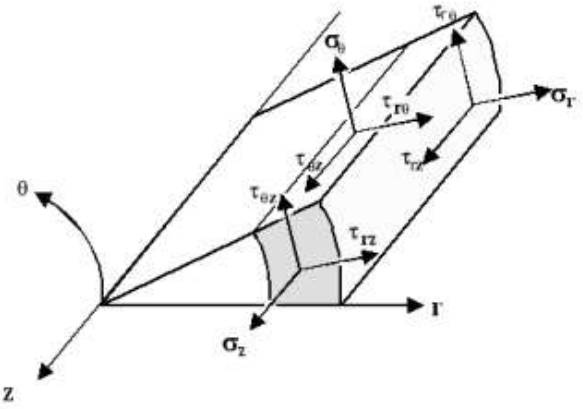

Fig. 3. Stress components in cylindrical coordinates.

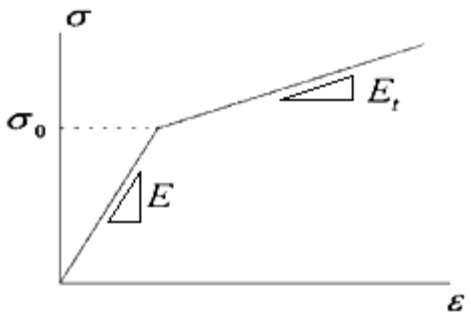

Fig. 4. Idealized stress-strain curve for linear hardening materials [25].

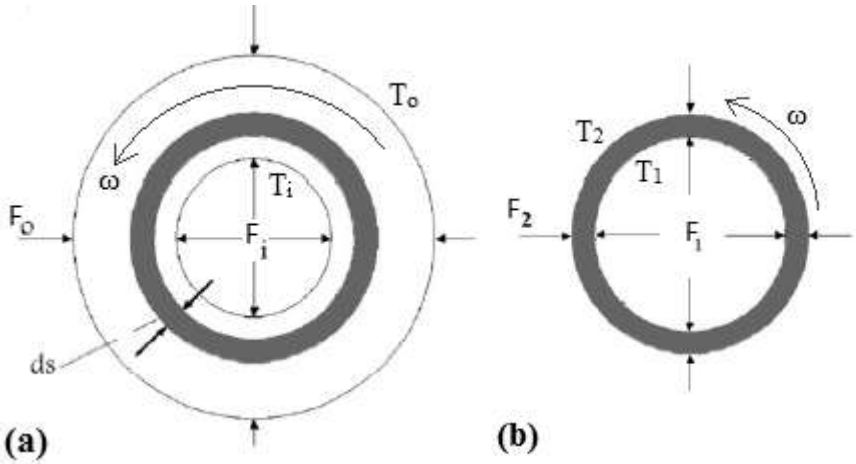

Fig. 5. (a) Rotating disk with boundary condition, (b) a ring of rotating disk with its boundary condition.

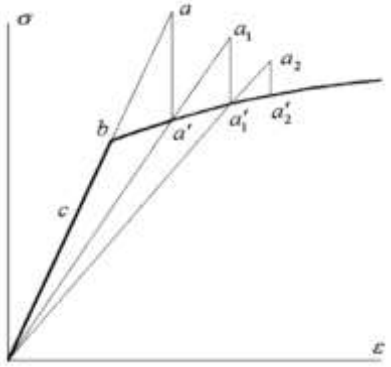

Fig. 6. Projection method.

ISSN 2349-4506
Impact Factor: 2.265

Global Journal of Engineering Science and Research Management

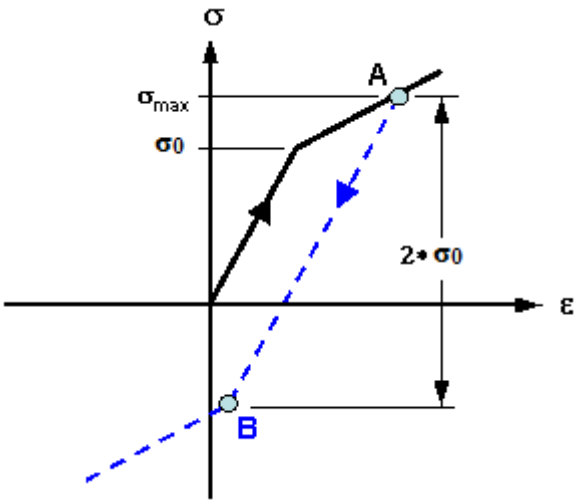

Fig.7. The conventional bilinear model with kinematic hardening.

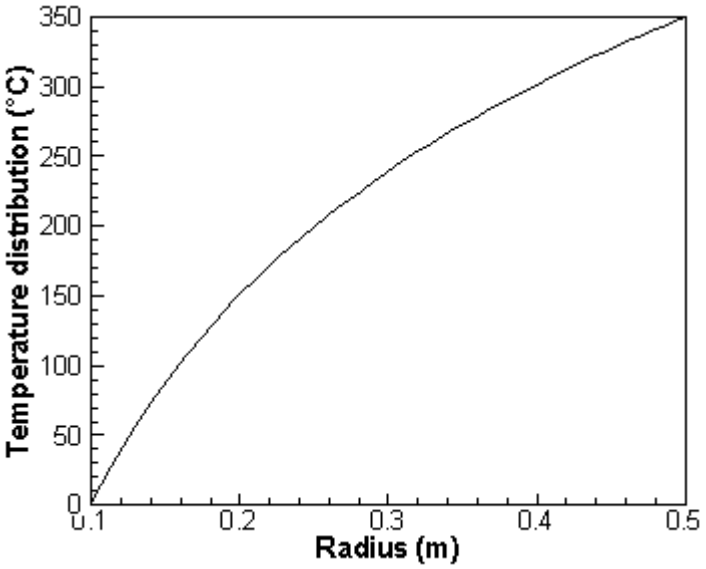

Fig. 8. Steady state temperature distribution of rotating disk.

ISSN 2349-4506
Impact Factor: 2.265

Global Journal of Engineering Science and Research Management

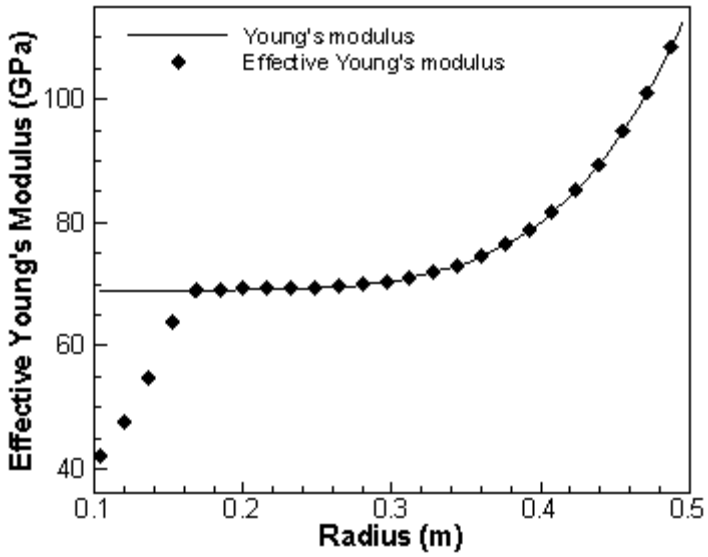

Fig. 9. The effective Young's modulus of disk under thermo-mechanical boundary conditions along the radius.

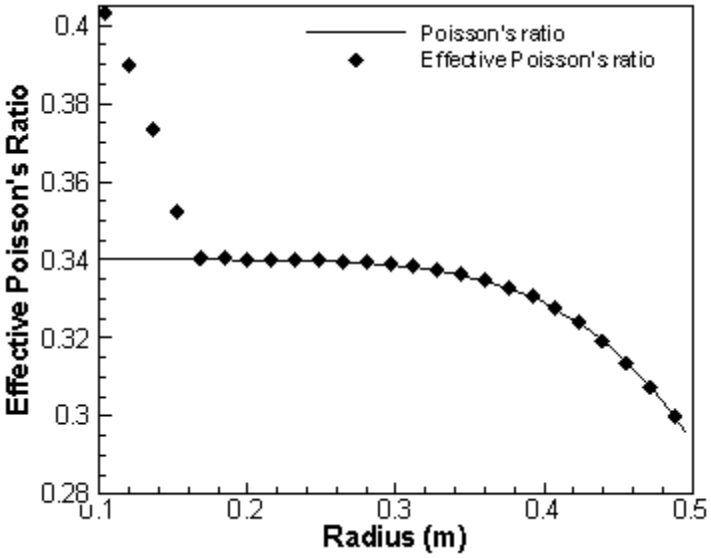

Fig. 10. The effective Poisson's ratio of disk under thermo-mechanical boundary conditions along the radius.

ISSN 2349-4506
Impact Factor: 2.265

Global Journal of Engineering Science and Research Management

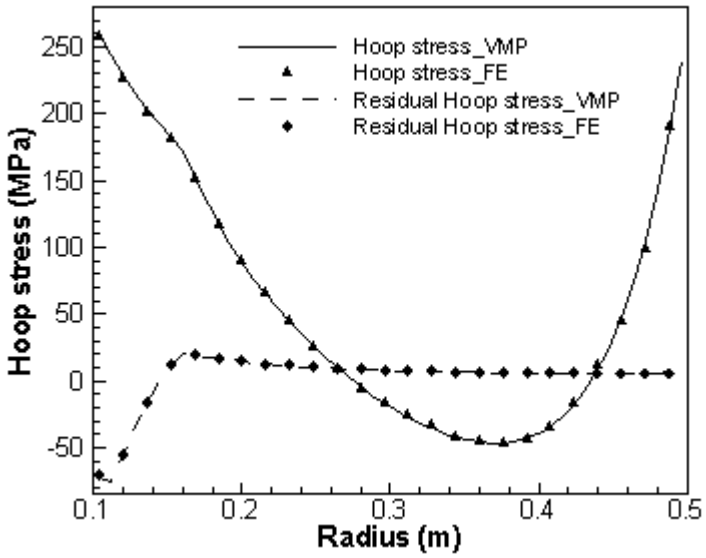

Fig. 11. Comparison of hoop and residual hoop stresses between the finite element method and VMP.

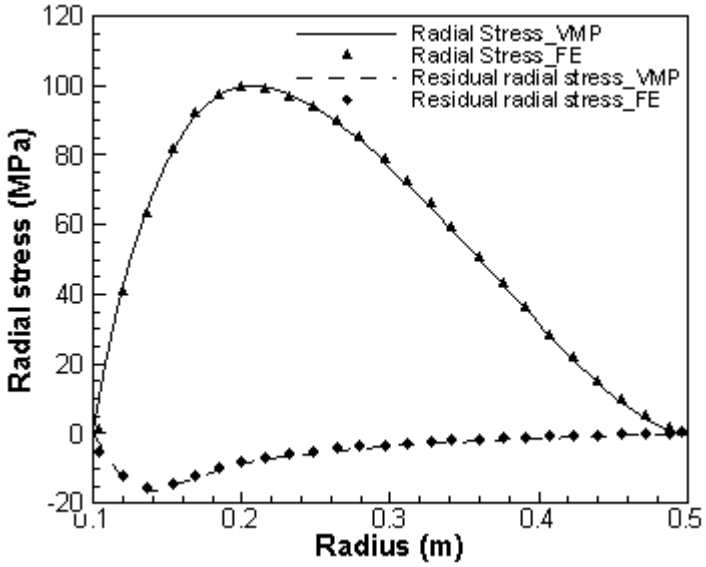

Fig. 12. Comparison of radial and residual radial stresses between the finite element method and VMP.

ISSN 2349-4506
Impact Factor: 2.265
Global Journal of Engineering Science and Research Management

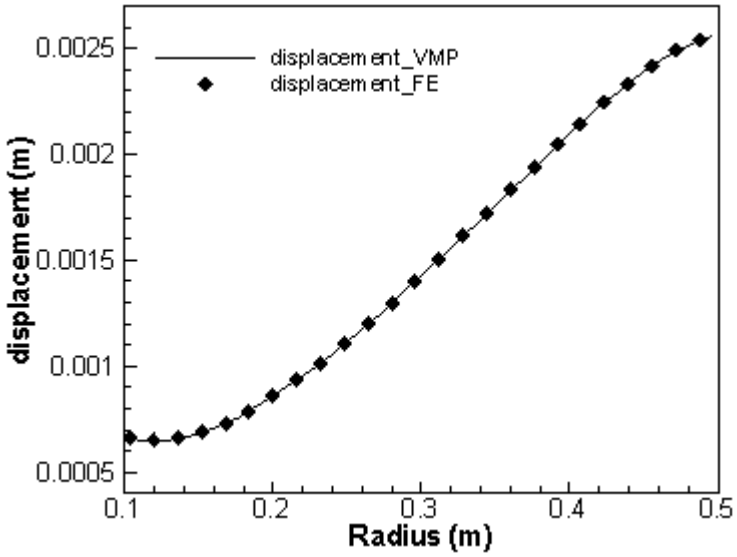

Fig. 13. Comparison of displacement between the finite element method and VMP .

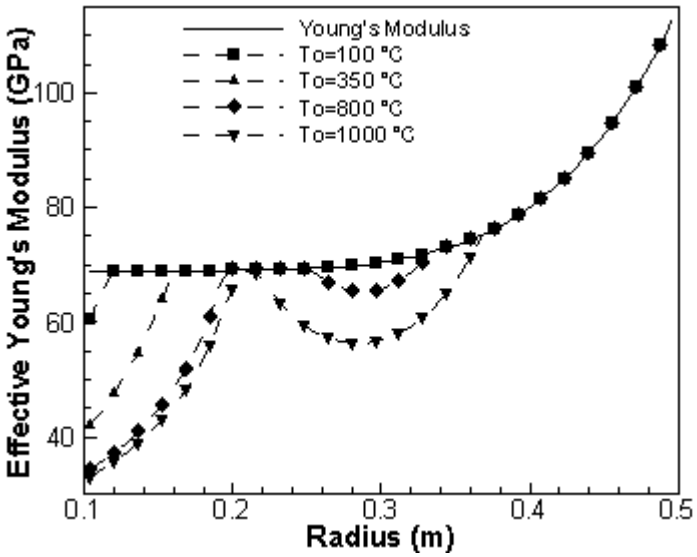

Fig. 14. Effect of temperature gradient changes on the effective Young's modulus of FG rotating disk.

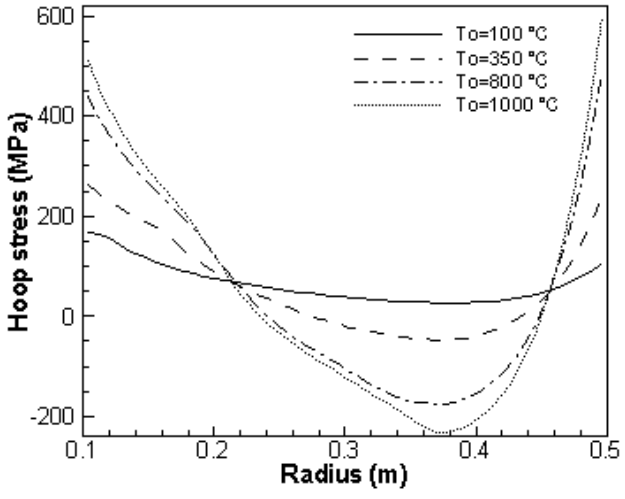

Fig. 15. Effect of temperature gradient changes on the hoop stresses of FG rotating disk.

ISSN 2349-4506
Impact Factor: 2.265
Global Journal of Engineering Science and Research Management

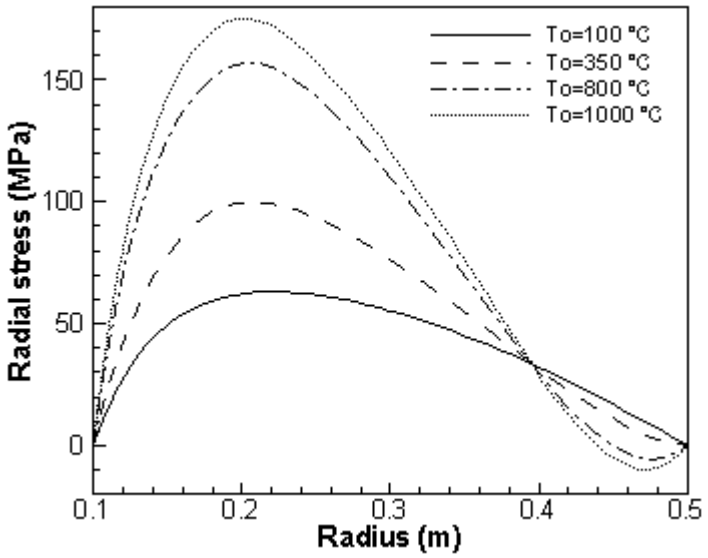

Fig. 16. Effect of temperature gradient changes on the radial stresses of FG rotating disk.

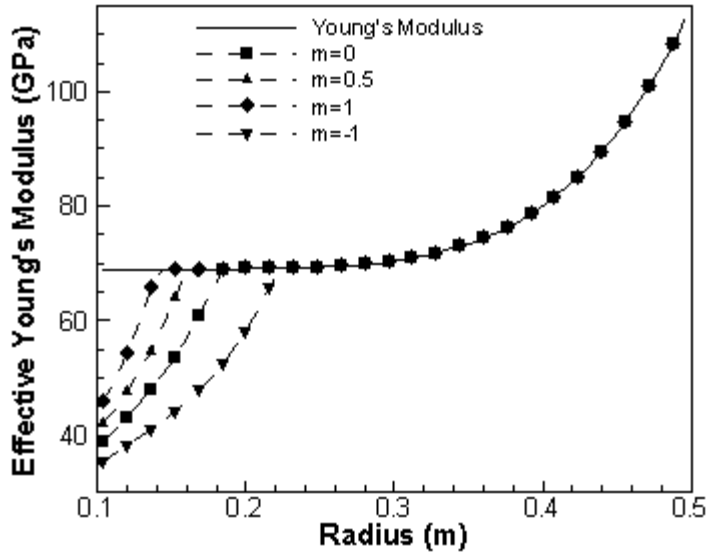

Fig. 17. Effect of thickness profile change on the effective Young's modulus of the FG rotating disk.

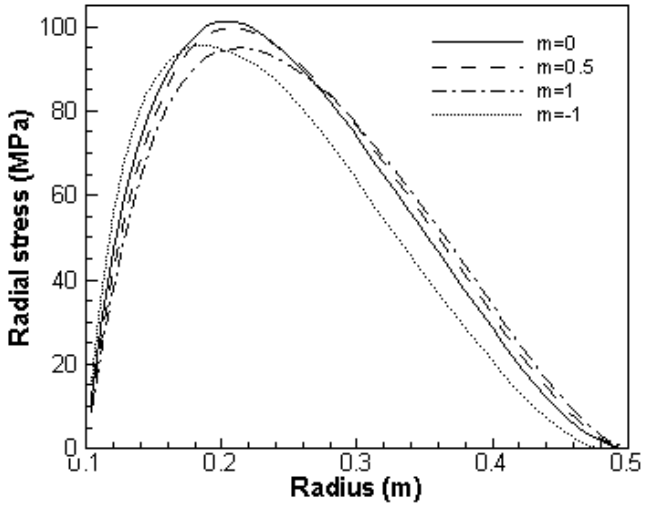

Fig. 18. Effect of thickness profile changes on the radial stress of FG rotating disk.

ISSN 2349-4506
Impact Factor: 2.265

Global Journal of Engineering Science and Research Management

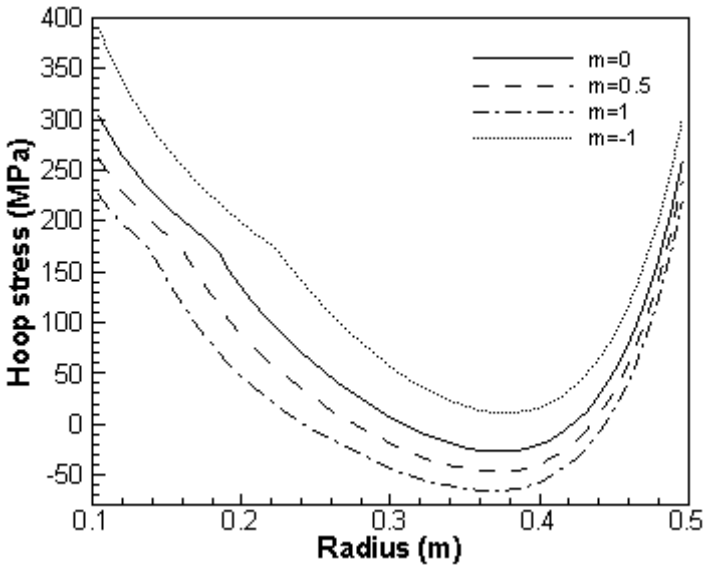

Fig. 19. Effect of thickness profile changes on the hoop stress of FG rotating disk.

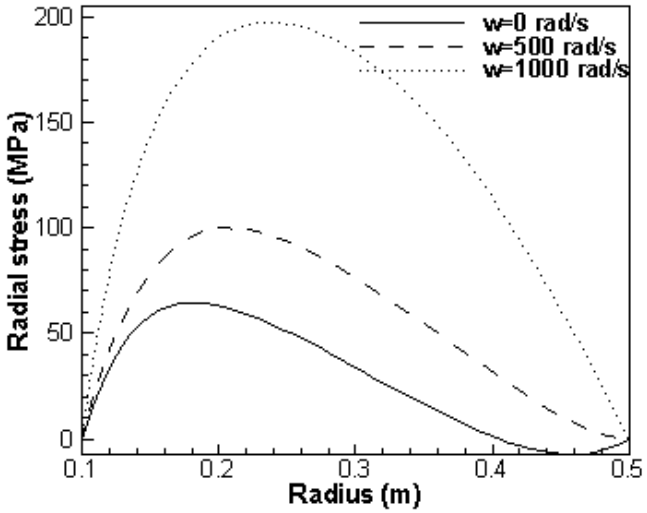

Fig. 20. Effect of angular velocity changes on the radial stress of FG rotating disk.

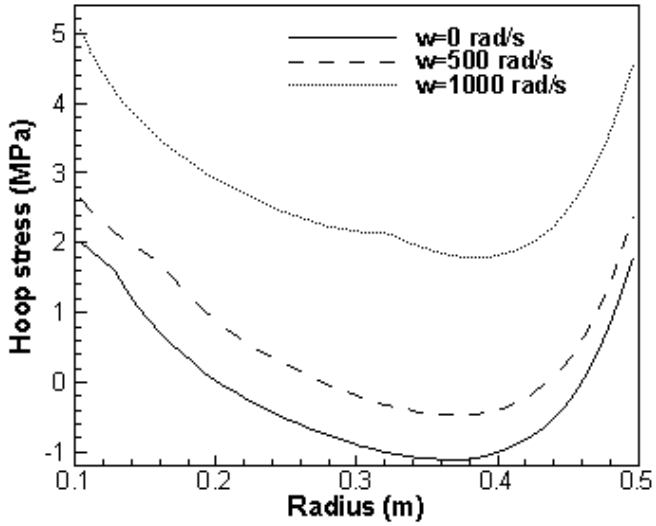

Fig. 21. Effect of angular velocity changes on the hoop stress of FG rotating disk.

ISSN 2349-4506
Impact Factor: 2.265
Global Journal of Engineering Science and Research Management

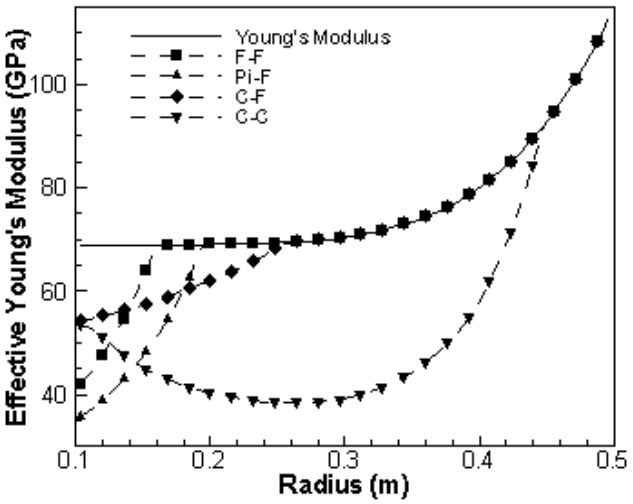

Fig. 22. Effect of different boundary conditions on the effective Young's modulus of FG rotating disk.

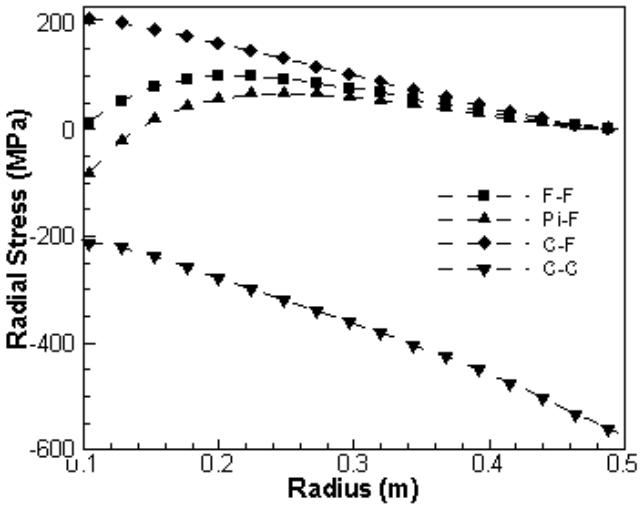

Fig. 23. Effect of boundary conditions on the radial stress of FG rotating disk.

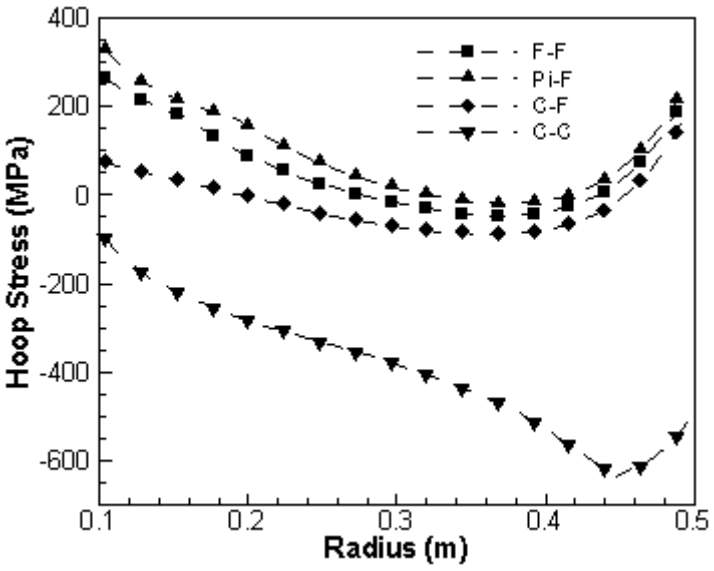

Fig. 24. Effect of boundary conditions on the hoop stress of FG rotating disk.

ISSN 2349-4506
Impact Factor: 2.265

Global Journal of Engineering Science and Research Management

Table 1 Properties of constituents of FG rotating disk.

	Young's modulus (GPa)	Tangent modulus (GPa)	Poisson's ratio	Density (kg/m^3)	Yield strength (MPa)	Thermal expansion coefficient ($1/°C$)
mat_1	69	27	0.34	2715	150	23×10^{-6}
mat_2	115	57	0.293	4515	1030	8×10^{-6}